

# Syntheses and Crystal Structures of Trigonal Rare-Earth Dioxymonocyanamides, $Ln_2O_2CN_2$ ( $Ln = Ce, Pr, Nd, Sm, Eu, Gd$ )

Yasuhiro Hashimoto, Masao Takahashi,<sup>1</sup> Shinichi Kikkawa, and Fumikazu Kanamaru

*The Institute of Scientific and Industrial Research, Osaka University, 8-1 Mihogaoka, Ibaraki, Osaka 567, Japan*

Received July 24, 1995; in revised form April 8, 1996; accepted April 25, 1996

New compounds, trigonal rare-earth dioxymonocyanamides  $Ln_2O_2CN_2$ , were synthesized by heating  $Ln_2O_3$  ( $Ln = Nd, Sm, Eu, Gd$ ),  $Ce_2(CO_3)_3 \cdot 8H_2O$ , or  $Pr_6O_{11}$  in the presence of carbon under flowing ammonia gas. The crystal structures of  $Ln_2O_2CN_2$  were refined by the Rietveld method using X-ray diffraction data. The  $Ln_2O_2CN_2$  compounds crystallize in the trigonal space group  $P\bar{3}m1$ , with  $a$  and  $c$  parameters varying from 3.9442 to 3.7812 Å and from 8.3609 to 8.2311 Å, respectively, as  $Ln$  atoms change from Ce to Gd. A choice of the space group was done assuming that the structure of  $Ln_2O_2CN_2$  is like that of  $Ln_2O_2S$ . In this paper, structural parameters for both  $Ce_2O_2CN_2$  and  $Gd_2O_2CN_2$  are not reported because the parameters for the atoms did not converge to reasonable values. These compounds have the layer structures which consist of the  $Ln_2O_2^{2+}$  layers with the interlayer  $CN_2^-$  ions. The  $Ln_2O_2^{2+}$  layers are piled perpendicular to the  $c$  axis and the linear cyanamide ions,  $^-N=C=N^-$ , are inserted parallel to the  $c$  axis. © 1996 Academic

Press, Inc.

## INTRODUCTION

Some kinds of the rare-earth compounds have a feature characterized by the layer structure. For example,  $LnOX$  ( $X = \text{halogen}$ ),  $Ln_2O_2Y$  ( $Y = \text{chalcogen}$ ), and  $Ln_2O_2CO_3$  belong to this kind of the compounds. These compounds consist of the  $Ln_2O_2^{2+}$  layers and the interlayer anions. They crystallize in the trigonal (or hexagonal) and/or the tetragonal form depending on the interlayer anions. Only  $CO_3^{2-}$  has been known as the polyatomic interlayer anion. In our study, a series of compounds,  $Ln_2O_2CN_2$  which contain other polyatomic anion have been synthesized. These compounds have the tetragonal and the trigonal structure depending on the  $Ln^{3+}$  ionic radii (1). The synthesis and the crystal structure refined by the Rietveld method of  $La_2O_2CN_2$  which crystallizes in the tetragonal structure have been already reported (2). In this paper, the syntheses and the crystal structures of the trigonal  $Ln_2O_2CN_2$  are reported.

<sup>1</sup> To whom correspondence should be addressed.

## EXPERIMENTAL

The trigonal  $Ln_2O_2CN_2$  were prepared by heating  $Pr_6O_{11}$  or  $Ln_2O_3$  ( $Ln = Nd, Sm, Gd$ ) at 1223 K for 12 h in a graphite boat under flowing ammonia gas. The reaction condition is the same as that for the preparation of  $La_2O_2CN_2$  (tetragonal) (2). In the case of  $Ln = Ce$ ,  $Ce_2(CO_3)_3 \cdot 8H_2O$  was heated at 1273 K. For  $Ln = Eu$ ,  $Eu_2O_3$  was calcined at 1023 K because the sample melted above 1023 K. Chemical compositions of the products were determined by CHN analyses and weight changes upon oxidizing the products to the corresponding oxides. Densities of the products were measured using pycnometry. IR spectra were recorded on a Hitachi spectrophotometer using the KBr method. Powder X-ray diffraction data were collected using a Rigaku RAD-RB diffractometer fitted with a graphite-monochromator employing  $CuK\alpha_1$  radiation. All powder X-ray diffraction data were refined by the Rietveld method using RIETAN (5, 6). The diffraction data were collected in steps of  $0.02^\circ$  over a range of  $20^\circ$ – $100^\circ$  in  $2\theta$ . Thermal analysis data were obtained on a Rigaku TAS-100 using a heating rate of 10 K/min in the temperature region between the room temperature and 1473 K.

## RESULTS AND DISCUSSION

The result of the CHN analysis of the product produced from  $Nd_2O_3$  indicated that the amounts of C, H, and N were 3.3, 0.0, and 7.6 wt%, respectively. After heating the sample above 1323 K in air, it decomposed into  $Nd_2O_3$  with a weight loss of 6.6%. The chemical formula of the product was determined to be  $Nd_2O_2CN_2$ . Values of C, N, and O contents calculated as  $Nd_2O_2CN_2$  are consistent with those obtained by the chemical and the thermal analysis. The same procedures were carried out for other products, and the chemical formula  $Ln_2O_2CN_2$  was obtained for all compounds (see Table 1). The N atoms in  $Ln_2O_2CN_2$  came from  $NH_3$  gas and the C atoms from the graphite boat. It is thought that the C atoms in the graphite boat react with  $NH_3$  gas, vaporize, and then react with the rare-earth

**TABLE 1**  
**Comparison between the Experimental and the Calculated**  
**Values of C, N, and O in  $Ln_2O_2CN_2$**

	C (wt%)	N (wt%)	O (wt%)	Weight loss (%)
	Ce			
Experimental	3.5 <sup>a</sup>	7.8 <sup>a</sup>	9.2 <sup>b</sup>	2.3
Calculated	3.4	8.0	9.1	2.3
	Pr			
Experimental	3.4 <sup>a</sup>	7.8 <sup>a</sup>	9.0 <sup>b</sup>	3.6
Calculated	3.4	7.9	9.0	3.8
	Nd			
Experimental	3.3 <sup>a</sup>	7.6 <sup>a</sup>	9.0 <sup>b</sup>	6.6
Calculated	3.3	7.8	8.9	6.7
	Sm			
Experimental	3.2 <sup>a</sup>	7.4 <sup>a</sup>	8.6 <sup>b</sup>	6.3
Calculated	3.2	7.5	8.6	6.4
	Eu			
Experimental	3.2 <sup>a</sup>	7.5 <sup>a</sup>	7.8 <sup>b</sup>	5.7
Calculated	3.2	7.4	8.5	6.4
	Gd			
Experimental	3.2 <sup>a</sup>	7.3 <sup>a</sup>	7.9 <sup>b</sup>	5.9
Calculated	3.1	7.2	8.3	6.2

<sup>a</sup> The values were obtained by CHN analysis.

<sup>b</sup> Oxygen contents were determined by weight losses on oxidation of the samples to the corresponding oxides and CHN analysis data.

oxides or carbonate because the graphite boat corrodes by heating under flowing ammonia gas. At first, the syntheses were carried out by using only the graphite boat as the carbon source. However, the sample had to be heated twice in order to obtain a single phase. The active charcoal in an alumina boat was placed at the upper end of the stream of the ammonia gas, since it was assumed that a larger quantity of carbon would cause the starting material to readily produce the desired products in one heating. The single phases were obtained by heating once at the above mentioned temperature for  $Ln = Ce$  to  $Eu$ . However,  $Gd_2O_3$  had to be heated twice even though this reaction system was used.

Figure 1 shows the IR spectra of  $Ln_2O_2CN_2$ . All IR spectra of  $Ln_2O_2CN_2$  show two absorption peaks in the vicinity of 670 and 1950  $cm^{-1}$ . These absorption peaks were assigned to the  $\nu_2$  and  $\nu_3$  modes of the  $CN_2^{2-}$  ion which were comparable to the IR spectrum of  $La_2O_2CN_2$  (2). The IR spectra of  $Ln_2O_2CN_2$  indicate that the trigonal  $Ln_2O_2CN_2$  also contain  $CN_2^{2-}$  ions.

When  $CeO_2$  was used as a starting material, the product was a mixture of  $Ce_2O_2CN_2$ ,  $CeO_2$ ,  $Ce_2O_3$ , and  $Ce_2ON_2$ . The stable oxide for Ce is  $CeO_2$  in which Ce is tetravalent. To synthesize  $Ce_2O_2CN_2$  from  $CeO_2$ ,  $Ce^{4+}$  has to be re-

duced to  $Ce^{3+}$  but it does not occur fully under the reaction condition used for this study. Therefore  $Ce_2(CO_3)_3 \cdot 8H_2O$  containing  $Ce^{3+}$  was chosen as a starting material. In the case of  $Pr_6O_{11}$  with a mixed valence state of  $Pr^{3+}$  and  $Pr^{4+}$ , the conversion from  $Pr_6O_{11}$  to  $Pr_2O_2CN_2$  occurred smoothly.

The powder X-ray diffraction patterns of  $Ln_2O_2CN_2$  could not be identified by using JCPDS data (7). All the diffraction peaks of each sample were indexed using the trigonal cell with the  $a$  and  $c$  parameters listed in Table 3 for  $Ln = Pr, Nd, Sm,$  and  $Eu$ , which were obtained by the Rietveld refinement which is mentioned later. The cell parameters for  $Ln = Ce$  and  $Gd$  were obtained by least square;  $a = 3.9441(7)$ ,  $c = 8.361(2)$  Å for  $Ln = Ce$ , and  $a = 3.7813(2)$ ,  $c = 8.2323(5)$  Å for  $Ln = Gd$ . The CELL package of programs (8) were used for indexing. The observed  $d$  values are in good agreement with those calculated as shown in Table 2.  $Nd_2O_2CN_2$  is presented, and the others may be obtained from the authors. The observed density of  $Nd_2O_2CN_2$  is 5.55  $g/cm^3$ , which is in good agreement with the calculated value of 5.52  $g/cm^3$  at  $Z = 1$ .

The powder X-ray diffraction patterns exhibit no system-

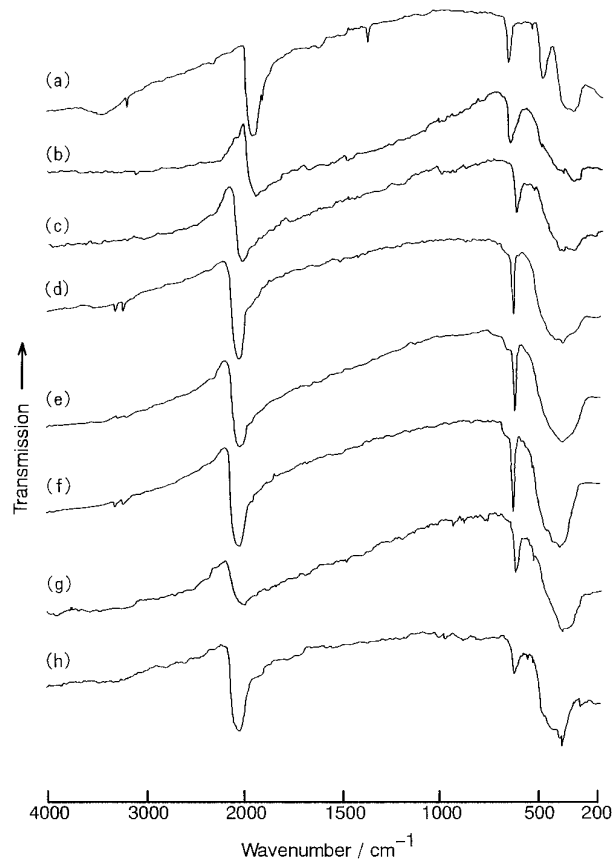


**FIG. 1.** Infrared spectra of  $Ln_2O_2CN_2$ , (a)La, (b)Ce (tetragonal), (c)Ce (trigonal), (d)Pr, (e)Nd, (f)Sm, (g)Eu, (h)Gd.

TABLE 2  
Powder X-Ray Diffraction Data for  $\text{Nd}_2\text{O}_2\text{CN}_2$

<i>h k l</i>	$d_{\text{obs}}$ (Å)	$d_{\text{cal}}$ (Å)	$I_{\text{obs}}/I_0$	$I_{\text{cal}}/I_0$
0 0 1	8.333	8.311	28	—
0 0 2	4.158	4.155	19	19
1 0 0	3.364	3.364	17	16
1 0 1	3.118	3.118	100	98
0 0 3	2.770	2.770	17	17
1 0 2	2.614	2.614	38	39
1 0 3	2.138	2.138	22	22
0 0 4	2.077	2.078	1	1
1 1 0	1.9415	1.9420	30	29
1 1 1	1.8907	1.8911	7	7
1 0 4	1.7670	1.7676	23	23
1 1 2	1.7593	1.7593	11	11
2 0 0	1.6815	1.6818	3	2
0 0 5	1.6614	1.6621	2	2
2 0 1	1.6479	1.6484	15	15
1 1 3	1.5896	1.5902	19	19
2 0 2	1.5585	1.5590	9	8
1 0 5	1.4895	1.4901	6	6
2 0 3	1.4370	1.4376	5	5
1 1 4	1.4181	1.4187	1	1
0 0 6	1.3845	1.3851	1	2
2 0 4	1.3066	1.3072	8	8
1 0 6	1.2802	1.2808	4	4
2 1 0	1.2709	1.2713	2	2
1 1 5	1.2622	1.2628	5	5
2 1 1	1.2563	1.2567	12	12
2 1 2	1.2153	1.2157	8	7
0 0 7	1.1818	1.1872	3	<1
2 0 5	1.1551	1.1822	5	3
2 1 3	1.1272	1.1555	5	5
1 1 6	1.1207	1.1277	4	5
3 0 0	1.1182	1.1212	6	4
1 0 7	1.1107	1.1195	1	5
3 0 1	1.1107	1.1111	1	1
2 1 4	1.0840	1.0844	11	9
3 0 2	1.0688	1.0825	2	2
2 0 6	1.0688	1.0692	2	2
3 0 3	1.0390	1.0393	6	5
0 0 8	1.0129	1.0388	<1	1
1 1 7	1.0129	1.0129	<1	<1
2 1 5	1.0095	1.0098	4	4

atic extinctions. Therefore the space group of these compounds could be any of the following hexagonal groups,  $P\bar{6}$ ,  $P6/m$ ,  $P622$ ,  $P6mm$ ,  $P\bar{6}m2$ ,  $P\bar{6}2m$ ,  $P6/mmm$ , or in one of the following trigonal groups,  $P3$ ,  $P\bar{3}$ ,  $P312$ ,  $P321$ ,  $P3m1$ ,  $P31m$ ,  $P\bar{3}1m$ ,  $P\bar{3}m1$ . Assuming that the crystal structure of the trigonal  $\text{Ln}_2\text{O}_2\text{CN}_2$  is similar to that of  $\text{Ln}_2\text{O}_2\text{S}$  with a trigonal symmetry which consists of the  $\text{Ln}_2\text{O}_2^{2+}$  layers and  $\text{S}^{2-}$ 's located between the layers, where the refinement of the structure was carried out by the Rietveld method.

In the structural model which consists of the  $\text{Ln}_2\text{O}_2^{2+}$  layers with the interlayer  $\text{CN}_2^{2-}$  ions, the refinement of the atomic coordinates and the isotropic thermal factors led to the lowest  $R$  factor when  $P\bar{3}m1$  was adopted. The structures were therefore refined with space group  $P\bar{3}m1$  with the structure model  $\text{Ln}$  at  $2d$  ( $\frac{1}{3}, \frac{2}{3}, z_1$ ) with  $z_1 \approx 0.18$ , O at  $2d$  ( $\frac{1}{3}, \frac{2}{3}, z_2$ ) with  $z_2 \approx 0.89$ , C at  $1b$  ( $0, 0, \frac{1}{2}$ ), and N at  $2c$  ( $0, 0, z_3$ ) with  $z_3 \approx 0.35$ . No preferred orientations were corrected. Figure 2 illustrates the profile fit and the difference pattern for  $\text{Nd}_2\text{O}_2\text{CN}_2$ . The solid line is calculated intensities, plus dots overlying the line are observed intensities, and  $\Delta y_i$  is the difference between the observed and the calculated intensities. Figure 2 shows that the calculated pattern fits the observed pattern very well. Tables 3 and 4 list the results of the Rietveld refinement and Table 5 presents interatomic distances. The definitions of the  $R$  factors in Table 3 can be seen in Ref. (9). The thermal parameters for the atoms in  $\text{Ce}_2\text{O}_2\text{CN}_2$  did not converge to the reasonable values which can be attributed to poor crystal growth of  $\text{Ce}_2\text{O}_2\text{CN}_2$ . As for  $\text{Ln} = \text{Gd}$ , the C–N distance obtained by the Rietveld refinement was 1.40 Å, which deviates significantly from 1.26–1.30 Å obtained for  $\text{Ln} = \text{Pr}, \text{Nd}, \text{Sm}, \text{and Eu}$ . If this value is correct, the wavenumbers of the  $\nu_2$  and  $\nu_3$  modes of the  $\text{CN}_2^{2-}$  ion in the IR spectrum for  $\text{Gd}_2\text{O}_2\text{CN}_2$  would differ greatly from those of other  $\text{Ln}_2\text{O}_2\text{CN}_2$ , but such a change is not observed in Fig. 1. It is guessed that  $\text{Ce}_2\text{O}_2\text{CN}_2$  and  $\text{Gd}_2\text{O}_2\text{CN}_2$  have the same structure as the others. A neutron diffraction study is now being carried out in order to determine the positions of the C and the N atoms. Therefore in this paper, the results of the Rietveld refinement for  $\text{Ln} = \text{Ce}$  and  $\text{Gd}$  are excluded.

Several inorganic cyanamides have been reported, such as  $\text{Na}_2\text{CN}_2$  (10),  $\text{PbCN}_2$  (11), and  $\text{CaCN}_2$  (12). There are two types of the  $\text{CN}_2^{2-}$  ions; one has two equivalent double bonds, C=N, and the other has C–N and C≡N bonds which have different distances between the C and the N atoms. In  $\text{CaCN}_2$ , both C–N distances are 1.25 Å, indicat-

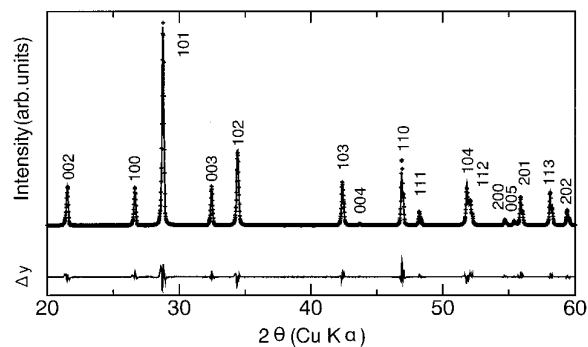


FIG. 2. Observed (++++ ) and calculated (—) powder X-ray diffraction pattern of  $\text{Nd}_2\text{O}_2\text{CN}_2$ . The difference profile appears below at the same scale.

TABLE 3  
Results of the Rietveld Refinement for the Trigonal  $Ln_2O_2CN_2$

	Pr	Nd	Sm	Eu
Cell dimension (Å)	$a = 3.9139(10)$ $c = 8.3324(15)$	$a = 3.8840(7)$ $c = 8.3106(12)$	$a = 3.8276(9)$ $c = 8.2666(15)$	$a = 3.8049(6)$ $c = 8.2515(9)$
Volume (Å <sup>3</sup> )	110.5	108.6	104.9	103.5
Calculated density (g/cm <sup>3</sup> )	5.32	5.51	5.90	6.04
$R_{wp}$	0.135	0.142	0.156	0.159
$R_p$	0.097	0.102	0.115	0.111
$R_B$	0.020	0.024	0.027	0.038
$R_F$	0.011	0.013	0.016	0.024
$S = R_{wp}/R_e$	2.18	2.24	2.44	2.36

Note. Space group is  $P\bar{3}m1$ , and  $Z$  is 1.  $R_{wp} = [\sum w_i(y_i(\text{obs}) - y_i(\text{calc}))^2 / (\sum w_i y_i(\text{obs})^2)]^{1/2}$ .  $R_p = (\sum |y_i(\text{obs}) - y_i(\text{calc})|) / \sum y_i(\text{obs})$ .  $R_B = (\sum |I_K(\text{obs}') - I_K(\text{calc})|) / \sum I_K(\text{obs}')$ .  $R_F = (\sum |I_K(\text{obs}')^{1/2} - I_K(\text{calc})^{1/2}|) / \sum I_K(\text{obs}')^{1/2}$ .  $R_e = [(N - P) / \sum w_i y_i(\text{obs})]^{1/2}$  (Ref. 9).

ing that there are two double bonds in the symmetrical  $\text{N}=\text{C}=\text{N}$  ion. In  $\text{H}_2\text{N}-\text{C}\equiv\text{N}$ , the bond distance of one C–N bond is 1.31 Å and another is 1.15 Å. Similarly  $\text{PbCN}_2$  has two different C–N bonds, i.e., 1.25 and 1.17 Å. In both cases of  $\text{CaCN}_2$  and  $\text{H}_2\text{N}-\text{C}\equiv\text{N}$ , the N–C–N group is linear, while as for  $\text{PbCN}_2$ , the N–C–N angle is  $177^\circ 30'$ , which deviates slightly from linearity. In  $Ln_2O_2CN_2$ , the  $\text{CN}_2^{2-}$  ion has two equivalent double bonds and is linear. The value of C=N distances in  $Ln_2O_2CN_2$  are 1.26–1.30 Å, which are similar to the C–N distance

in  $\text{CaCN}_2$ , 1.25 Å (12). Our results also support the existence of cyanamide ions in  $Ln_2O_2CN_2$ .

Figure 3 illustrates the crystal structure of the trigonal  $Ln_2O_2CN_2$ . The structures of the  $Ln_2O_2^{2+}$  layers in the trigonal  $Ln_2O_2CN_2$  are similar to those of the trigonal or the hexagonal  $Ln_2O_2X$  ( $X = \text{S}$  (13, 14),  $\text{Se}$  (15),  $\text{CO}_3$  (16)). In  $Ln_2O_2CN_2$ ,  $Ln^{3+}$ 's are slightly stuck out of the  $O^{2-}$  plane toward the outside from the central plane of the  $Ln_2O_2^{2+}$  layers. The  $Ln_2O_2^{2+}$  layers are laid perpendicular to the  $c$  axis and the linear  $\text{CN}_2^{2-}$  ions are inserted parallel to the

TABLE 4  
Structural Parameters for the Trigonal  $Ln_2O_2CN_2$  in  $P\bar{3}m1$   
( $T = \text{Room temperature}$ )

Atom	Site	$g$	$x$	$y$	$z$	$B(\text{Å}^2)$
Pr						
Pr	$2d$	1.0	$\frac{1}{3}$	$\frac{2}{3}$	0.1819(9)	0.4(1)
O	$2d$	1.0	$\frac{1}{3}$	$\frac{2}{3}$	0.892(6)	0.9(14)
C	$1b$	1.0	0	0	$\frac{1}{2}$	2.3(44)
N	$2c$	1.0	0	0	0.346(9)	1.6(16)
Nd						
Nd	$2d$	1.0	$\frac{1}{3}$	$\frac{2}{3}$	0.1811(8)	0.4(1)
O	$2d$	1.0	$\frac{1}{3}$	$\frac{2}{3}$	0.893(6)	1.0(13)
C	$1b$	1.0	0	0	$\frac{1}{2}$	3.8(49)
N	$2c$	1.0	0	0	0.349(9)	1.3(16)
Sm						
Sm	$2d$	1.0	$\frac{1}{3}$	$\frac{2}{3}$	0.180(1)	0.4(2)
O	$2d$	1.0	$\frac{1}{3}$	$\frac{2}{3}$	0.882(7)	1.2(15)
C	$1b$	1.0	0	0	$\frac{1}{2}$	3.5(52)
N	$2c$	1.0	0	0	0.345(10)	0.8(17)
Eu						
Eu	$2d$	1.0	$\frac{1}{3}$	$\frac{2}{3}$	0.180(1)	0.3(2)
O	$2d$	1.0	$\frac{1}{3}$	$\frac{2}{3}$	0.887(6)	0.2(13)
C	$1b$	1.0	0	0	$\frac{1}{2}$	0.7(37)
N	$2c$	1.0	0	0	0.342(12)	1.8(19)

TABLE 5  
Interatomic Distances in the Trigonal  $Ln_2O_2CN_2$  in Å

	Pr	Nd	Sm	Eu
$Ln-O$	2.34(1)	2.32(1)	2.27(1)	2.26(1)
$Ln-N$	2.64(4)	2.64(4)	2.59(4)	2.57(5)
$C-N$	1.28(8)	1.26(7)	1.29(9)	1.30(10)

$c$  axis. The coordination number of  $Ln^{3+}$  is 7. The orientation of the linear  ${}^{-}N=C=N^{-}$  ion does not deviate from the parallel to the  $c$  axis. N atom would have a larger thermal parameter in the position used in this analysis if the  ${}^{-}N=C=N^{-}$  chain was inclined at some degrees.  $Ln^{3+}$  is surrounded by four oxygen and three nitrogen atoms.  $Ln^{3+}$  exists on the plane formed by three oxygen atoms, another oxygen atom locates under or over  $Ln^{3+}$ , and three nitrogen atoms form a plane parallel to the plane formed by  $Ln^{3+}$  and three oxygen atoms. On the other hand, in the tetragonal  $Ln_2O_2CN_2$ , the Rietveld analysis of the powder X-ray diffraction pattern revealed that the  $Ln_2O_2^{2+}$  layers are perpendicular to the  $c$  axis, and the  $CN_2^{2-}$  ions are perpendicular to the  $c$  axis, i.e., parallel to the  $Ln_2O_2^{2+}$  layers. The coordination number of  $Ln^{3+}$  is 8. The  $Ln^{3+}$  is surrounded by four oxygen atoms on the same plane and statistically four nitrogen atoms which are located on the same plane against the  $Ln_2O_2^{2+}$  layers (2).

The  $\nu_2$  (bending) and  $\nu_3$  (antisymmetric stretch) modes of  ${}^{-}N=C=N^{-}$  in IR spectra shift in the trigonal structure

when compared to the tetragonal structure (Fig. 1b and 1c). In the trigonal structure, the  $\nu_2$  mode shifts to lower wavenumber and the  $\nu_3$  mode shifts to higher wavenumber when compared to the tetragonal phase. The differences in the wavenumbers of the  $\nu_2$  and the  $\nu_3$  modes between the tetragonal and the trigonal structures are 25 and 100  $cm^{-3}$ , respectively. The shift of the  $\nu_2$  mode indicates that the bending of the  ${}^{-}N=C=N^{-}$  ion in the trigonal structure occurs more easily than in the tetragonal structure. It is thought that the  $\nu_3$  mode is influenced by  $Ln^{3+}$ 's bond to N atoms. One N atom is surrounded by four  $Ln^{3+}$ 's in the tetragonal phase (2) and three in the trigonal phase. Therefore, the Coulomb force between the rare-earth and nitrogen atoms in the trigonal structure is less than that in the tetragonal structure, so the interaction between C and N is stronger and the  $\nu_3$  mode shifts to higher wavenumber in the trigonal structure.

Figure 4 shows the TG-DTA curve for  $Nd_2O_2CN_2$ . The measurement was carried out in air. The weight of sample begins to increase at about 923 K accompanied by an exothermic DTA peak. The curve shows a maximum weight gain at about 973 K and afterward shows a large decrease in weight. The weight of sample becomes constant at about 1323 K. The sample heated at about 1323 K was found to be  $Nd_2O_3$  by X-ray diffraction. At the temperature where the weight of the sample is at a maximum, it was found by X-ray diffraction that the hexagonal  $Nd_2O_2CO_3$  was produced. The results of the TG-DTA measurement and X-ray diffraction indicates that the interlayer anion  $CN_2^{2-}$  is oxidized to  $CO_3^{2-}$  by heating in air. The exothermic

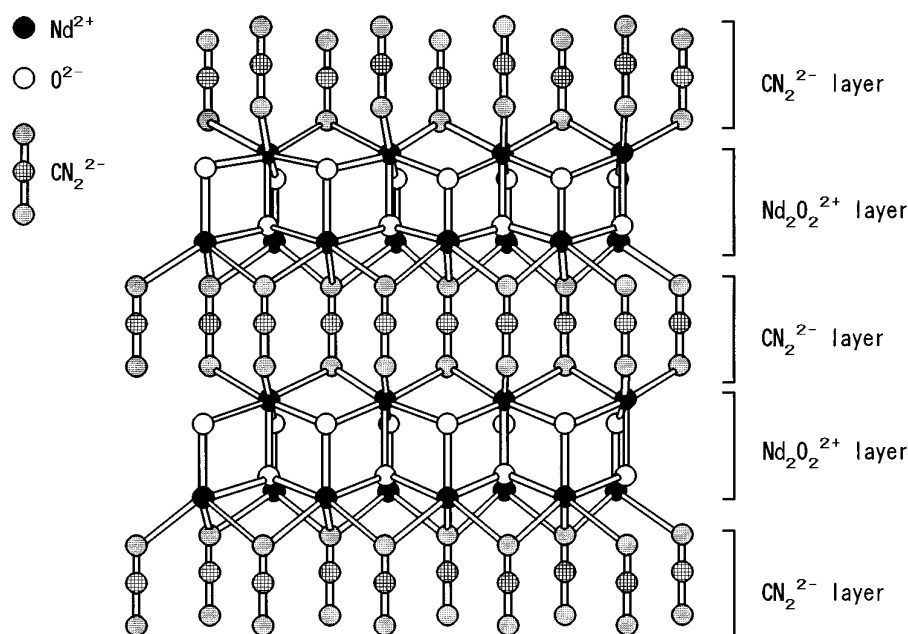


FIG. 3. Crystal structure of  $Nd_2O_2CN_2$ .

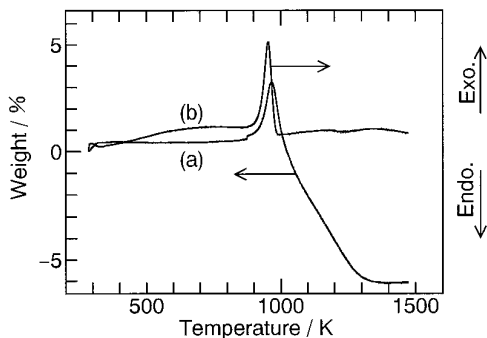


FIG. 4. (a)TG and (b)DTA curve for  $\text{Nd}_2\text{O}_2\text{CN}_2$ .

DTA peak at about 973 K is due to the oxidation of  $\text{CN}_2^{2-}$  to  $\text{CO}_3^{2-}$ . In addition to  $\text{Ln} = \text{Nd}$ , other  $\text{Ln}_2\text{O}_2\text{CN}_2$  showed similar TG-DTA curves. The temperatures where the oxidations begin are 603, 803, 923, 943, 993, and 993 K for Ce, Pr, Nd, Sm, Eu, and Gd, respectively. The temperature increases remarkably with decreasing ionic radii of  $\text{Ln}^{3+}$ .  $\text{Ln}_2\text{O}_2\text{S}$  also become  $\text{Ln}_2\text{O}_2\text{SO}_4$  by heating in air. In this case, the interlayer anion  $\text{S}^{2-}$  is oxidized to  $\text{SO}_4^{2-}$  and the crystal structures change from the trigonal ( $\text{Ln}_2\text{O}_2\text{S}$ ) to the orthorhombic ( $\text{Ln}_2\text{O}_2\text{SO}_4$ ) structure (17).

Supplementary materials have been deposited and may also be obtained from the authors.

### CONCLUSION

The crystal structures of the trigonal  $\text{Ln}_2\text{O}_2\text{CN}_2$  were analyzed by the Rietveld refinement of the powder X-ray diffraction pattern. The trigonal  $\text{Ln}_2\text{O}_2\text{CN}_2$  crystallize in the space group  $P\bar{3}m1$  ( $Z = 1$ ). It was found that these compounds consist of the  $\text{Ln}_2\text{O}_2^{2+}$  layers with the interlayer  $\text{CN}_2^{2-}$  ions. The IR spectra of the trigonal and the tetragonal  $\text{Ln}_2\text{O}_2\text{CN}_2$  indicate that the coordination of  $\text{Ln}^{3+}$  atoms around nitrogen atoms are different in each structure type. Because of the layer structure, the interlayer  $\text{CN}_2^{2-}$  ion is

oxidized to  $\text{CO}_3^{2-}$  by heating in air. The structures of the trigonal  $\text{Ln}_2\text{O}_2\text{CN}_2$  are closely related to those of the trigonal  $\text{Ln}_2\text{O}_2\text{X}$  ( $X = \text{S}, \text{Se}$ ) and the hexagonal  $\text{Ln}_2\text{O}_2\text{X}$  ( $X = \text{CO}_3$ ) which consist of the  $\text{Ln}_2\text{O}_2^{2+}$  layers and the interlayer anions.

### ACKNOWLEDGMENT

The present work was partially supported by a Grant-in Aid for Scientific Research from the Ministry of Education, Science, and Culture of Japan, and also the Scientific Research Grant-in Aid for Special Project Research, "Advanced Materials Creation and their Limit State Prediction for Environmental Preservation" from Osaka University. The authors are grateful to Ms. F. Fukuda and Dr. Y. Miyamoto of ISIR, Osaka University for the compositional analyses, and Mr. H. Yamada of Material Analysis Center of ISIR for IR spectra measurements.

### REFERENCES

1. Y. Hashimoto, M. Takahashi, S. Kikkawa, and F. Kanamaru, *Chem. Lett.*, 1963 (1994).
2. Y. Hashimoto, M. Takahashi, S. Kikkawa, and F. Kanamaru, *J. Solid State Chem.* **114**, 592 (1995).
3. R. Ballestracci, *C. R. Seances Acad. Sci. Ser. B* **264**, 1736 (1967).
4. J. O. Sawyer, P. Caro, and L. Eyring, *Monatsh. Chem.* **102**, 333 (1971).
5. F. Izumi, "The Rietveld Method" (R. A. Young, Ed.), Chap. 13. Oxford University Press, Oxford, 1993.
6. Y.-I. Kim and F. Izumi, *J. Ceram. Soc. Jpn.* **102**, 401 (1994).
7. Joint Committee on Powder Diffraction Standards "Powder Diffraction Files," International Centre for Diffraction Data, Pennsylvania.
8. Y. Takaki, T. Taniguchi, and K. Hori, *J. Ceram. Soc. Jpn.* **101**, 373 (1993).
9. R. A. Young, "The Rietveld Method" (R. A. Young, Ed.), Chap. 1. Oxford University Press, Oxford, 1993.
10. K. N. Adams, M. J. Cooper, and M. J. Sole, *Acta Crystallogr.* **17**, 1449 (1964).
11. M. J. Cooper, *Acta Crystallogr.* **17**, 1452 (1964).
12. Y. Yamamoto, K. Kinoshita, K. Tamaru, and T. Yamanaka, *Bull. Chem. Soc. Jpn.* **31**, 501 (1958).
13. W. H. Zachariasen, *Acta Crystallogr.* **2**, 60 (1949).
14. H. A. Eick, *J. Am. Chem. Soc.* **80**, 43 (1958).
15. H. A. Eick, *Acta Crystallogr.* **13**, 161 (1960).
16. A. N. Christensen, *Acta Chem. Scand.* **24**, 2440 (1970).
17. J. W. Haynes and J. J. Brown, Jr., *J. Electrochem. Soc.* **115**, 1060 (1968).